The phase-field approach to brittle fracture: A tutorial on the theory and the numerical implementation

1 Variational theory of brittle fracture for crack propagation

Griffith's (1921) main conceptual tenet for crack propagation was a cost-benefit analysis of the state of the crack — the crack length along a pre-assigned crack path — at any given time. In other words, the Griffith's idea states that the crack has a given length at that time because having a longer crack would cost more surface energy that it would save in potential energy. As a consequence, he derived the notion of critical energy release rate as a necessary first order condition for his initial postulate. As such, the infamous $G \leq G_c$ was a mere by-product of Griffith's viewpoint.

The intention of Francfort and Marigo (1998) and others in developing the variational theory for brittle fracture was to readjust the focus of fracture mechanics to be more in line with Griffith's original intent. In their theory, the fracture state is viewed as a minimization problem for the sum of the potential and surface energies with arbitrary add-cracks as test fields. There is no need to appeal to the notion of energy release rate or stress intensity factors. At the same time, an additional ingredient, energy conservation, forces crack evolution.

In the most basic setting, that of an isotropic linear elastic material with stored-energy function $W(\mathbf{E}) := 1/2\{2\mu\mathbf{E}\cdot\mathbf{E} + \lambda(\mathrm{tr}\ \mathbf{E})^2\}$ occupying an open bounded domain $\Omega \subset \mathbb{R}^N, N = 1, 2, 3$, the evolution, discretized in time for simplicity, goes as follows. Denote by G_c the critical elastic energy release rate or fracture toughness and assume that $\overline{\mathbf{u}}$ is a time-dependent displacement prescribed on a part $\partial\Omega_{\mathcal{D}}$ of the boundary. Then the displacement field $\mathbf{u}_k = \mathbf{u}_k(\mathbf{x})$ and crack set Γ_k within Ω at any given discrete time $t_k \in \{0 = t_0, t_1, ..., t_m, t_{m+1}, ..., t_M = T\}$ is determined by the minimization problem

$$(\mathbf{u}_k, \Gamma_k) = \underset{\substack{\mathbf{u}=\overline{\mathbf{u}}(t_k)\,\mathrm{on}\,\partial\Omega_{\mathcal{D}}\setminus\Gamma \\ \Gamma\supset\Gamma_{k-1}}}{\arg\min} \mathcal{E}(\mathbf{u},\Gamma) := \int_{\Omega\setminus\Gamma} W(\mathbf{E}(\mathbf{u}))\,\mathrm{d}\mathbf{x} + G_c\mathcal{H}^{N-1}\left(\Gamma\cap\overline{\Omega}\setminus\partial\Omega_{\mathcal{N}}\right). \tag{1}$$

In this expression, $\mathcal{H}^{N-1}(\Gamma)$ stands for the $(N-1)$–dimensional Hausdorff measure (the surface measure) of the unknown crack Γ, $\partial\Omega_{\mathcal{N}} = \partial\Omega \setminus \partial\overline{\Omega}_{\mathcal{D}}$, and $\mathbf{E}(\mathbf{u}) := 1/2(\nabla\mathbf{u} + \nabla\mathbf{u}^T)$ for the symmetrized gradient of the displacement field $\mathbf{u}$.

2 Phase-field regularization of variational theory

The minimization problem above is not suitable for numerical implementation. However, it is amenable to approximation through regularized formulations that are often labeled "phase-field" approximations (Bourdin et al., 2000). We introduce a phase field

$$v = v(\mathbf{X}, t)$$

taking values in $[0, 1]$. Precisely, $v = 1$ identifies regions of the sound material, whereas, in the limit as a regularization length scale $\varepsilon \searrow 0$, $0 \leq v < 1$ identifies regions of the material that have been fractured. Then, the regularized minimization problems is given by

$$(\mathbf{u}_k^\varepsilon, v_k^\varepsilon) = \underset{\substack{\mathbf{u}=\overline{\mathbf{u}}(t_k)\,\mathrm{on}\,\partial\Omega_{\mathcal{D}} \\ 0\leq v\leq v_{k-1}\leq 1}}{\arg\min} \mathcal{E}^\varepsilon(\mathbf{u},v) := \int_\Omega \psi(v)W(\mathbf{E}(\mathbf{u}))\,\mathrm{d}\mathbf{x} + \frac{G_c}{4c_s}\int_\Omega\left(\frac{s(v)}{\varepsilon} + \varepsilon\nabla v\cdot\nabla v\right)\mathrm{d}\mathbf{x}, \tag{2}$$

where ψ and s are continuous monotonic functions such that $\psi(0) = 0$, $\psi(1) = 1$, $s(0) = 1$, $s(1) = 0$, and $c_s := \int_0^1 \sqrt{s(z)}\mathrm{d}z$ is a normalization parameter; see, e.g., Braides (1998). The best and most commonly used choice now for functions ψ and s is nowadays referred to as the AT1 model:

$$\psi(v) = v^2 \qquad \text{and} \qquad s(v) = 1 - v. \tag{3}$$

However, this choice is one of a plethora of possible choices that can be used. The key is that the regularized problem should converge in an energetic sense (Γ convergence) to the sharp problem. Braides (1998) discusses different approximations for the area of $(N-1)$–dimensional surfaces contained in N-dimensional domains. The specific form form has the merit that it is mathematically simple, it leads to sharp transitions of the phase-field variable from $v = 1$ to $v = 0$, and possesses a number of other theoretical advantages over another popular form (called AT2 model) in which,

$$\psi(v) = v^2 \qquad \text{and} \qquad s(v) = (1 - v)^2.$$

For more discussion on this matter, we refer to Pham et al. (2011).

The Euler-Lagrange equations for the regularized problem can be written as the following, solving for the displacement field $\mathbf{u}_k(\mathbf{X}) = \mathbf{u}(\mathbf{X}, t_k)$ and phase field $v_k(\mathbf{X}) = v(\mathbf{X}, t_k)$ at any material point $\mathbf{X} \in \overline{\Omega}$ and discrete time $t_k \in \{0 = t_0, t_1, ..., t_m, t_{m+1}, ..., t_M = T\}$:

$$\begin{cases} \mathrm{Div}\left[v_k^2 \dfrac{\partial W}{\partial \mathbf{E}}(\mathbf{E}(\mathbf{u}_k))\right] = \mathbf{0}, \quad \mathbf{X} \in \Omega, \\ \mathbf{u}_k = \overline{\mathbf{u}}(\mathbf{X}, t_k), \quad \mathbf{X} \in \partial\Omega_{\mathcal{D}}, \\ \left[v_k^2 \dfrac{\partial W}{\partial \mathbf{E}}(\mathbf{E}(\mathbf{u}_k))\right] \mathbf{N} = \overline{\mathbf{t}}(\mathbf{X}, t_k), \quad \mathbf{X} \in \partial\Omega_{\mathcal{N}} \end{cases} \tag{4}$$

and

$$\begin{cases} \varepsilon\, G_c \triangle v_k = \dfrac{8}{3} v_k W(\mathbf{E}(\mathbf{u}_k)) - \dfrac{G_c}{2\varepsilon}, \text{if } v_k(\mathbf{X}) < v_{k-1}(\mathbf{X}), \quad \mathbf{X} \in \Omega \\ \varepsilon\, G_c \triangle v_k \geq \dfrac{8}{3} v_k W(\mathbf{E}(\mathbf{u}_k)) - \dfrac{G_c}{2\varepsilon}, \text{if } v_k(\mathbf{X}) = 1 \ \text{ or } \ v_k(\mathbf{X}) = v_{k-1}(\mathbf{X}) > 0, \quad \mathbf{X} \in \Omega \\ v_k(\mathbf{X}) = 0, \quad \text{if } v_{k-1}(\mathbf{X}) = 0, \quad \mathbf{X} \in \Omega \\ \nabla v_k \cdot \mathbf{N} = 0, \quad \mathbf{X} \in \partial\Omega \end{cases} \tag{5}$$

with $\mathbf{u}(\mathbf{X}, 0) \equiv \mathbf{0}$ and $v(\mathbf{X}, 0) \equiv 1$, where $\nabla \mathbf{u}_k(\mathbf{X}) = \nabla \mathbf{u}(\mathbf{X}, t_k)$, $\nabla v_k(\mathbf{X}) = \nabla v(\mathbf{X}, t_k)$, $\triangle v_k(\mathbf{X}) = \triangle v(\mathbf{X}, t_k)$. The inequalities in the second PDE exist because of the constraint that phase-field remains between 0 and 1 and moreover is non-increasing (assuming fracture is irreversible, dissipative process.) The inequalities in the second PDE can be removed by the use of a penalty method:

$$\begin{cases} \mathrm{div}\left[\varepsilon\, G_c \nabla v_k\right] = \dfrac{8}{3} v_k W(\mathbf{E}(\mathbf{u}_k)) - \dfrac{G_c}{2\varepsilon} + \dfrac{8\,\zeta}{3}\, p(v_{k-1}, v_k), & \mathbf{X} \in \Omega \\ \nabla v_k \cdot \mathbf{N} = 0, & \mathbf{X} \in \partial\Omega \end{cases} \tag{6}$$

with

$$p(v_{k-1}, v_k) = \mathcal{H}\left(v_\alpha - v_k\right)\left(|v_{k-1} - v_k| - (v_{k-1} - v_k)\right) + |1 - v_k| - (1 - v_k) - |v_k| + v_k, \tag{7}$$

Here, $\mathcal{H}(\cdot)$ stands for the Heaviside function and v_α denotes the value below which the phase field v is considered to be non-increasing in time. Also, the regularization parameter ζ should be selected to be large relative to term $G_c/2\varepsilon$. Typical value assumed is $\zeta = 10^3 G_c/(2\varepsilon)$.

3 Shortcomings of the classical phase-field model

3.1 Inability to describe nucleation

It is well known from experimental data that in the absence of a large pre-existing crack, crack nucleation or initiation is necessarily governed by the material's strength. Yet, the classical phase-field model has no information about strength in it.

Consider an example of a homogeneous bar without any defects subjected to uniaxial tension. For $\varepsilon \searrow 0$, the above classical phase-field model would predict that the bar would break at an infinite applied stress. However, for a finite value of ε, the bar would break at a finite value of applied stress. This observation from a one-dimensional example has led numerous authors to promote the idea that a meaningful nucleation can be obtained by fixing the value of ε to the "right" length scale. As an example, Tanné et al. (2018) suggests that for the AT1 model, the localization length for a material with Young's modulus E, tensile strength $\sigma_{\mathtt{ts}}$, and critical energy release rate G_c can be set to the following value to include the information about strength in the classical phase-field model:

$$\varepsilon = \frac{3G_cE}{8\sigma_{\mathtt{ts}}^2}. \tag{8}$$

However, this approach suffers from various shortcomings. First, fixing the value of localization length means that the resulting model is no longer a fracture model, but rather forms a damage model. Furthermore, as discussed in the next section, strength is defined as a set of critical stresses that form a surface in the stress space. The above approach of tying up the value of ε to the tensile strength $\sigma_{\mathtt{ts}}$ (or to any other single strength data point for that matter) of a given material of interest arbitrarily privileges a *single* point on the strength surface while ignoring the rest of that surface.

Moreover, the above approach is intrinsically inadequate to model nucleation under arbitrary homogeneous stress state conditions because it is fundamentally based on an energy criterion and not a stress criterion. To illustrate this, consider an example of a spherical ball made out of an incompressible material subjected to spherically symmetric tensile loading. The above approach, despite how the value of ε is set, will always predict that the ball would fracture at an infinite stress because strain energy in the ball prior to fracture is zero.

3.2 Behavior under compression

The classical phase-field model does not distinguish between tension and compression due to its energetic nature. Energy is released due to fracture in both tension and compression which is physically unrealistic. Consider as an example the three point bending test with an arbitrary brittle material. The classical phase-field would not predict fracture from the notch, but rather in the region under the point load or near the supports.

4 The basic ingredients for the modeling of fracture nucleation

Experimental results indicate that macroscopic crack nucleation in homogeneous brittle materials falls into one of the three different types schematically depicted in Fig. 1; see, e.g., Irwin (1958). Any attempt at a comprehensive macroscopic theory of fracture nucleation should convincingly handle all three.

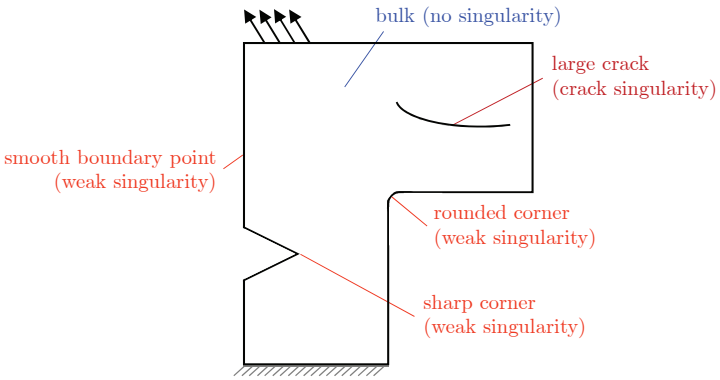

Fig. 1: Schematic of a structure made of a homogeneous brittle material under general quasistatic boundary conditions. Fracture may nucleate: *i*) at material points in the bulk, *ii*) from large pre-existing cracks, or *iii*) from the boundary, be it straight or be it a corner, or small pre-existing cracks.

3.1 Nucleation in the bulk: The strength.

Brittle materials contain inherent defects of mostly micron and submicron size. When a specimen made of a brittle material is subjected to a state of monotonically increasing uniform stress, fracture will nucleate from one or more of those pre-existing defects at a finite critical value of the applied stress. The set of all such critical stresses defines a surface in stress space

$$\mathcal{F}(\boldsymbol{\sigma}) = 0, \tag{9}$$

which we refer to as the *strength surface* of the material. Experimental evidence points to the intrinsic character of such a surface, although it is observed to be stochastic partially due to the experimental difficulties in measuring strength. For materials whose elastic response is isotropic, it is reasonable to postulate that their strength surface is also isotropic. Then

$$\mathcal{F}(\boldsymbol{\sigma}) = \widetilde{\mathcal{F}}(\sigma_1, \sigma_2, \sigma_3) = \widehat{\mathcal{F}}\left(I_1, J_2, J_3\right) = 0, \tag{10}$$

where σ_1, σ_2, σ_3 stand for the principal stresses and

$$I_1 = \operatorname{tr} \boldsymbol{\sigma}, \quad J_2 = \frac{1}{2}\operatorname{tr} \boldsymbol{\sigma}_D^2, \quad J_3 = \frac{1}{3}\operatorname{tr} \boldsymbol{\sigma}_D^3 \quad \text{with} \quad \boldsymbol{\sigma}_D = \boldsymbol{\sigma} - \frac{1}{3}\left(\operatorname{tr} \boldsymbol{\sigma}\right)\mathbf{I} \tag{11}$$

denote the standard invariants.

3.2 Nucleation from large pre-existing cracks: The critical energy release rate

When the domain under investigation already contains a large[1] pre-existing crack, fracture may nucleate from the crack front. In other words, the crack may propagate. That the nucleation of fracture from large cracks in brittle materials is well described by the Griffith competition between bulk elastic energy and surface fracture energy is by now a settled matter. Roughly speaking, fracture may nucleate from a large pre-existing crack whenever the criterion

$$-\frac{\partial \mathcal{W}}{\partial \Gamma} = G_c$$

is satisfied, namely, whenever the change in potential energy $\mathcal{W}$ in the structure with respect to an added surface area Γ to the crack reaches the critical elastic energy release rate or fracture toughness G_c of the material.

[1] "Large" refers to large relative to the characteristic size of the inherent microscopic defects in the material under investigation. By the same token, "small" refers to sizes that are of the same order or just moderately larger than the sizes of the inherent defects.

3.3 Nucleation from the boundary and small pre-existing cracks: The transition zone

We view the case of a crack nucleating from a boundary point or a small pre-existing crack as the result of a mediation between strength and toughness. An abundance of experimental results for the nucleation of fracture emanating from smooth and sharp corners and from small cracks can be found in the literature, and this within a wide range of brittle materials. They suggest a transition from toughness-dominated regime to a strength-dominated regime based on the geometry of the macroscopic defect that creates stress concentration or stress singularity.

5 Revisited phase-field model to incorporate nucleation

Kumar et al. (2018a) have proposed a modification to the governing equations to incorporate the three different types of nucleation outlined in the previous section. The proposed modification is to include a driving force

$$c_{\mathsf{e}}(\mathbf{X}, t), \qquad (\mathbf{X}, t) \in \Omega \times [0, T]$$

in the Euler-Lagrange equation for the phase field $v(\mathbf{x}, t)$. Thus the resulting regularized equation for phase field reads as:

$$\begin{cases} \operatorname{div}\left[\varepsilon\, G_c \nabla v_k\right] = \dfrac{8}{3} v_k W(\mathbf{E}(\mathbf{u}_k)) - \dfrac{4}{3} c_{\mathsf{e}} - \dfrac{G_c}{2\varepsilon} + \dfrac{8\,\zeta}{3}\, p(v_{k-1}, v_k), & \mathbf{X} \in \Omega \\ \nabla v_k \cdot \mathbf{N} = 0, & \mathbf{X} \in \partial\Omega \end{cases} \tag{12}$$

Physically, the driving force c_{e} can be thought of as the macroscopic manifestation of the presence of the inherent microscopic defects in the material. Hence, it is the quantity that allow us to incorporate the material's strength surface into the model.

The driving force c_{e} is constructed as follows. The general recipe was first presented in Kumar et al. (2020). A simplified model for nucleation dominated by hydrostatic strength was presented in Kumar et al. (2018a,b) Based on experimental data, assume a particular form for the strength surface. A commonly utilized choice that fits experimental data well for a wide range of materials is the Drucker-Prager strength surface (Drucker and Prager, 1952):

$$\widehat{\mathcal{F}}(I_1, J_2) = \sqrt{J_2} + \gamma_1 I_1 + \gamma_0 = 0, \tag{13}$$

where γ_0 and γ_1 stand for material constants, and note that the procedure for other types of strength surfaces would not be fundamentally different.

Then, choose for c_{e} an identical functional form as the given strength surface but with ε-dependent coefficients that are suitably picked so that, in the limit as the localization length $\varepsilon \searrow 0$, the resulting phase-field model (4)–(5) predicts fracture nucleation in the bulk exactly according to the given strength surface. For Drucker-Prager strength surface, this principle leads to:

$$c_{\mathsf{e}}(\mathbf{X}, t) = \widehat{c}_{\mathsf{e}}(I_1, J_2; \varepsilon) = \beta_2^{\varepsilon} \sqrt{J_2} + \beta_1^{\varepsilon} I_1 + \beta_0^{\varepsilon} \tag{14}$$

The coefficients β_2^{ε} and β_1^{ε} are chosen for a particular value of ε so that the model agrees exactly with the Drucker-Prager strength surface at two points. These two points can be conveniently chosen to correspond to uniaxial tension and uniaxial compression. More precisely, this means that β_2^{ε} and β_1^{ε} can be obtained by solving the following algebraic equation under stress and strain conditions for uniaxial tension and compression:

$$\frac{8}{3} W(\mathbf{E}(\mathbf{u})) - \frac{4}{3}\left(\beta_2^{\varepsilon} \sqrt{J_2} + \beta_1^{\varepsilon} I_1 + \beta_0^{\varepsilon}\right) - \frac{G_c}{2\varepsilon} = 0, \tag{15}$$

for a given value of β_0^ε. We choose to define the third constant β_0^ε in terms of a unit-less coefficient δ^ε as

$$\beta_0^\varepsilon = \delta^\varepsilon \frac{3G_c}{8\varepsilon}.$$

Then the other coefficients are obtained as

$$\begin{cases} \beta_1^\varepsilon = -\left(\dfrac{(1+\delta^\varepsilon)(\sigma_{\mathtt{cs}} - \sigma_{\mathtt{ts}})}{2\sigma_{\mathtt{cs}}\sigma_{\mathtt{ts}}}\right)\dfrac{3G_c}{8\varepsilon} - \dfrac{\sigma_{\mathtt{cs}} - \sigma_{\mathtt{ts}}}{2E} \\ \beta_2^\varepsilon = -\left(\dfrac{\sqrt{3}(1+\delta^\varepsilon)(\sigma_{\mathtt{cs}} + \sigma_{\mathtt{ts}})}{2\sigma_{\mathtt{cs}}\sigma_{\mathtt{ts}}}\right)\dfrac{3G_c}{8\varepsilon} + \dfrac{\sqrt{3}(\sigma_{\mathtt{cs}} + \sigma_{\mathtt{ts}})}{2E} \end{cases},$$

The coefficient δ^ε needs to be calibrated so that nucleation from large pre-existing cracks is according to the Griffith principle. The calibration of the parameter δ^ε is what allows the governing equations to marry the concept of strength in the bulk with the concept of Griffith energy competition at crack singularities. In order to determine the correct value of δ^ε for a given finite localization length ε, we consider a boundary-value problem for which the nucleation from a large pre-existing crack can be determined exactly — according to Griffith's sharp theory of brittle fracture for linear elastic materials (LEFM) — and then have the phase-field model with external driving force match that exact solution thereby determining δ^ε.

A convenient problem to solve is the classical problem of a pre-existing crack of size $2a$ embedded at the center of a plate of width $2b$ and height $2L \geq 2b$ subject to a tensile force perpendicular to the crack. A simple exact asymptotic solution is available for this problem in the limit as $b \to \infty$. For finite b, Tada et al. (1973) reported the following approximate analytical solution (that differs from an exact power-series solution at most by 0.1%) for the critical applied stress $\sigma_{cr}^{\text{LEFM}}$ at which fracture nucleation occurs from the front of the pre-existing crack under plane-stress conditions:

$$\sigma_{cr}^{\text{LEFM}} = \frac{\sqrt{\cos\left(\dfrac{\pi a}{2b}\right)}}{1 - 0.025\left(\dfrac{a}{b}\right)^2 + 0.06\left(\dfrac{a}{b}\right)^4}\sqrt{\frac{G_c E}{\pi a}}, \tag{16}$$

A correction to $c_{\mathtt{e}}$ to handle singular compressive stresses for finite ε.

The above model, unlike the classical phase-field (Amor et al., 2009; Miehe et al., 2010), naturally models the tension-compression asymmetry of the fracture process. However, it leads to a predicted strength surface that does not match the Drucker-Prager strength surface well in stress states close to hydrostatic compression. This means that under singular compressive loads, e.g. near point loads, a very small value of ε needs to be chosen which makes computations expensive. To resolve this issue, Kumar et al. (2022) have proposed an $O(\varepsilon^0)$ correction to the formula for the driving force. The modified $c_{\mathtt{e}}$ reads as

$$c_{\mathtt{e}}(\mathbf{X}, t) = \beta_2^\varepsilon\sqrt{J_2} + \beta_1^\varepsilon I_1 + \beta_0^\varepsilon + \frac{1}{v^3}\left(1 - \frac{\sqrt{I_1^2}}{I_1}\right)\left(\frac{J_2}{2\mu} + \frac{I_1^2}{6(3\lambda + 2\mu)}\right). \tag{17}$$

In this expression,

$$\begin{cases} \beta_0^\varepsilon = \delta^\varepsilon \dfrac{3G_c}{8\varepsilon} \\ \beta_1^\varepsilon = -\left(\dfrac{(1+\delta^\varepsilon)(\sigma_{\mathtt{cs}} - \sigma_{\mathtt{ts}})}{2\sigma_{\mathtt{cs}}\sigma_{\mathtt{ts}}}\right)\dfrac{3G_c}{8\varepsilon} + \dfrac{\sigma_{\mathtt{ts}}}{6(3\lambda+2\mu)} + \dfrac{\sigma_{\mathtt{ts}}}{6\mu} \\ \beta_2^\varepsilon = -\left(\dfrac{\sqrt{3}(1+\delta^\varepsilon)(\sigma_{\mathtt{cs}} + \sigma_{\mathtt{ts}})}{2\sigma_{\mathtt{cs}}\sigma_{\mathtt{ts}}}\right)\dfrac{3G_c}{8\varepsilon} + \dfrac{\sigma_{\mathtt{ts}}}{2\sqrt{3}(3\lambda+2\mu)} + \dfrac{\sigma_{\mathtt{ts}}}{2\sqrt{3}\mu} \end{cases},$$

Note that the modified driving force is asymptotically identical in the limit as $\varepsilon \searrow 0$ to that utilized by Kumar et al. (2020). The calibration of the parameter δ^ε is conducted in an identical fashion as before.

6 Numerical implementation of the phase-field model

The numerical implementation of the classical and revisited phase-field models is exactly the same. The finite-element method is used to generate numerical solutions for the coupled system of equations. First, we reformulate the time-discretized governing equations in a weak form We look for the displacement field $\mathbf{u}_k \in \mathcal{U}$ and phase field $v_k \in W^{1,2}(\Omega_0)$ such that

$$\int_{\Omega_0} v_k^2 \frac{\partial W}{\partial \mathbf{E}}(\mathbf{E}(\mathbf{u}_k)) \cdot \nabla \mathbf{y} \, \mathrm{d}\mathbf{X} - \int_{\partial\Omega_0^{\mathbf{S}}} \bar{\mathbf{t}} \cdot \mathbf{y} \, \mathrm{d}\mathbf{X} = 0 \quad \forall \mathbf{y} \in \mathcal{U}_0, \, t \in [0,T] \tag{18}$$

and

$$\int_{\Omega_0} \left\{ \varepsilon \, G_c \nabla v_k \cdot \nabla p + \left[\frac{8}{3} v_k W(\mathbf{E}(\mathbf{u}_k)) + \frac{4}{3} c_{\mathtt{e}} - \frac{G_c}{2\varepsilon} + \frac{8}{3} p(v_{k-1}, v_k) \right] p \right\} \mathrm{d}\mathbf{X} = 0 \quad \forall p \in W^{1,2}(\Omega_0), \, t \in [0,T]. \tag{19}$$

where

$$\mathcal{U} = \left\{ \mathbf{y} \in W^{1,2}(\Omega_0; \mathbb{R}^N) : \mathbf{y} = \overline{\mathbf{u}} \text{ on } \partial\Omega_0^{\mathbf{y}} \right\}, \quad \mathcal{U}_0 = \left\{ \mathbf{y} \in W^{1,2}(\Omega_0; \mathbb{R}^N) : \mathbf{y} = \mathbf{0} \text{ on } \partial\Omega_0^{\mathbf{y}} \right\},$$

The weak form can be further discretized in space with FEM. For compressible material behavior, linear Lagrange elements can be used to discretize both the displacement field and the phase field. The space discretization has to fine enough to resolve the smallest length scale in the problem which is the localization length ε. A general rule of thumb for the AT1 model is that the FE mesh size has to $\varepsilon/5$ to resolve the length scale well, although a larger mesh size up to $\varepsilon/3$ can often be used. To save computational cost, mesh can be refined only in regions where a crack is expected to nucleate or propagate. For near incompressible material behavior, linear non-conforming elements (Crouzeix and Raviart, 1973) have been shown to be a suitable choice for the discretization of displacement field, see Kumar et al. (2018a) for more details.

The two resulting algebraic equations after space discretization needs to be solved with a staggered algorithm (also known as alternating minimization or fixed-point iteration method). In general, the two equations can not be solved in a monolithic fashion. In a staggered algorithm, at each time step, the two equations are solved one at a time iteratively, until convergence is reached (Bourdin et al., 2008). The convergence can be defined in terms of the residual of one or both of the equations or in some alternate way. The staggered algorithm, however, can be brutally slow to converge for many problems and improving its speed is a matter of active research.

References

Ambrosio, L., Tortorelli, V.M., 1990. Approximation of functionals depending on jumps by elliptic functionals via Γ-convergence. *Commun. Pure Appl. Math.* 43, 999–1036.

Amor, H., Marigo, J.-J., Maurini, C., 2009. Regularized formulation of the variational brittle fracture with unilateral contact: Numerical experiments. *Journal of the Mechanics and Physics of Solids* 57, 1209–1229.

Bourdin, B., Francfort, G.A., Marigo, J.J., 2000. Numerical experiments in revisited brittle fracture. *Journal of the Mechanics and Physics of Solids* 48, 797–826.

Bourdin, B., Francfort, G.A., Marigo, J.J., 2008. The variational approach to fracture. *Journal of Elasticity* 91, 5–148.

Braides, A., 1998. *Approximation of Free-Discontinuity Problems*. Springer.

Crouzeix, M., Raviart, P.-A., 1973. Conforming and nonconforming finite element methods for solving the stationary stokes equations I. *Rev. Française Automat. Informat. Recherche Opérationnelle. Mathématique* 7, 33–75.

Drucker, D.C., Prager, W., 1952. Soil mechanics and plastic analysis for limit design. *Quarterly of Applied Mathematics* 10, 157–165.

Francfort, G.A., Marigo, J.J., 1998. Revisiting brittle fracture as an energy minimization problem. *Journal of the Mechanics and Physics of Solids* 46, 1319–1342.

Griffith, A.A., 1921. The phenomena of rupture and flow in solids. *Philos. Trans. R. Soc. Lond. A* 221, 163–198.

Hossain, M.Z., Hsueh, C.-J., Bourdin, B., Bhattacharya, K., 2014. Effective toughness of heterogeneous media. *J. Mech. Phys. Solids* 71, 320–348.

Irwin, G., 1957. Analysis of stresses and strains near the end of a crack traversing a plate. *Journal of Applied Mechanics* 24, 361–364.

Kumar, A., Francfort, G.A., Lopez-Pamies, O., 2018a. Fracture and healing of elastomers: A phase-transition theory and numerical implementation. *Journal of the Mechanics and Physics of Solids* 112, 523–551.

Kumar, A., Ravi-Chandar, K., Lopez-Pamies, O., 2018b. The configurational-forces view of fracture and healing in elastomers as a phase transition. *International Journal of Fracture* 213, 1–16.

Kumar, A., Lopez-Pamies, O., 2020. The phase-field approach to self-healable fracture of elastomers: A model accounting for fracture nucleation at large, with application to a class of conspicuous experiments. *Theoretical and Applied Fracture Mechanics* 107, 102550.

Kumar, A., Bourdin, B., Francfort, G.A., Lopez-Pamies, O., 2020. Revisiting nucleation in the phase-field approach to brittle fracture. *Journal of the Mechanics and Physics of Solids* 142, 104027.

Kumar, A., Lopez-Pamies, O., 2021. The poker-chip experiments of Gent and Lindley (1959) explained. *Journal of the Mechanics and Physics of Solids* 150, 104359.

Kumar, A., Ravi-Chandar, K., Lopez-Pamies, O., 2022. The revisited phase-field approach to brittle fracture: Application to indentation and notch problems. *International Journal of Fracture* 237, 83–100.

Miehe, C., Welschinger, F., Hofacker, M., 2010. Thermodynamically consistent phase-field models of fracture: variational principles and multi-field FE implementations. *Int. J. Numer. Methods Eng.* 83, 1273–1311.

Pham, K., Amor, H., Marigo, J.J., Maurini, C., 2011. Gradient damage models and their use to approximate brittle fracture. *Int. J. Damage Mech.* 20, 618–652.

Rice, J.R., 1968. A path independent integral and approximate analysis of strain concentration by notches and cracks. *Journal of Applied Mechanics* 35, 379–386.

Tada, H., Paris, P. C., Irwin, G. R., 1973. *The Stress Analysis of Cracks Handbook 3rd Edition.* The American Society of Mechanical Engineers, New York.

Tanné, E., Li, T., Bourdin, B., Marigo, J.J., Maurini, C., 2018. Crack nucleation in variational phase-field models of brittle fracture. *Journal of the Mechanics and Physics of Solids* 110, 80–99.